Letter

Strongly correlated crystalline higher-order topological phases in two-dimensional systems: A coupled-wire study

Jian-Hao Zhang *

Department of Physics, The Chinese University of Hong Kong, Shatin, New Territories, Hong Kong, China and Department of Physics, The Pennsylvania State University, University Park, Pennsylvania 16802, USA

(Received 11 February 2022; revised 5 July 2022; accepted 11 July 2022; published 22 July 2022)

Coupled-wire constructions have been widely applied to quantum Hall systems and symmetry-protected topological (SPT) phases. In this Letter, we use the coupled one-dimensional nonchiral Luttinger liquids with domain-wall structured mass terms as quantum wires to construct crystalline higher-order topological superconductors (HOTSCs) in two-dimensional (2D) interacting fermionic systems by two representative examples: a D_4-symmetric class-D HOTSC and a C_4-symmetric class-BDI HOTSC, with Majorana corner modes on the edge. Furthermore, based on the coupled-wire constructions, the quantum phase transitions between different phases of 2D HOTSCs by tuning the interwire coupling are investigated in a straightforward way.

DOI: 10.1103/PhysRevB.106.L020503

Introduction. Topological phases of quantum matter have become one of the greatest triumphs of condensed matter physics since the discovery of the fractional quantum Hall effect [1,2]. Topological order defined by patterns of long-range entanglement provides a systematic way of understanding the topological phases of quantum matter [3]. Furthermore, the interplay between symmetry and topology plays a central role in the topological phases of quantum matter. In particular, symmetry-protected topological (SPT) phases have been systematically constructed and classified in short-range entangled systems [4–26]. An elegant example of SPT phases is a topological insulator, protected by time-reversal and charge-conservation symmetry [27,28]. Recently, crystalline SPT phases have been intensively studied [29–60], with great opportunities for experimental realizations [61–64]. In particular, different from internal SPT phases, the boundaries of two-dimensional (2D) crystalline SPT phases are almost gapped but with protected 0D *corner* zero modes. These types of topological phases are called *higher-order topological phases* [65–76].

The study of higher-order topological phases mainly focuses on free-fermion systems, because interactions and crystalline symmetries restrict the analytical study of the lattice model, and only the numerics on a finite-size lattice can give some insights. On the other hand, a clear and powerful tool for studying the topological phases of quantum matter is the coupled-wire construction [77–88]. One decomposes a higher-dimensional system into an assembly of 1D quantum wires, and topological properties then arise from the suitable couplings of them. A unique advantage of coupled-wire construction is that, different from the higher-dimensional quantum field theory, the powerful bosonization technique of one-dimensional subsystems can be used to challenge the strong interaction effects. Different phases are manifested by patterns of coupled wires and the quantum phase transition of different phases is controlled by tuning interwire couplings directly. Therefore, an important open question arises: Can strongly correlated higher-order topological phases be constructed from a coupled-wire perspective?

In this Letter, we systematically construct a crystalline higher-order topological superconductor (HOTSC) in two-dimensional interacting fermionic systems by coupling the circular 1D nonchiral Luttinger liquids with domain-wall structured mass terms as quantum wires, via two typical intriguing interacting examples, a D_4-symmetric class-D HOTSC and a C_4-symmetric class-BDI HOTSC, whose higher-order edge modes are Majorana zero modes (MZMs) [45,46]. By suitable interwire tunnelings/interactions, several 1D quantum wires are assembled and fully gapped, leaving a few dangling quantum wires at the edge or near the center of the systems. Near the center, the dangling quantum wires are fully gapped by intrawire interactions; on the edge, the dangling quantum wires explicitly manifest the higher-order topological edge modes of 2D HOTSCs by their domain-wall structure. Different 2D HOTSCs are characterized by different patterns of coupled wires. Lattice translation symmetry can also be imposed straightforwardly. Furthermore, with a concrete coupled-wire construction of a 2D HOTSC, we directly investigate the quantum phase transitions by tuning different coupling constants of interwire interactions. We stress that our arguments are not sensitive to a specific geometry of quantum wires: The calculations are applicable to any geometry respecting the specific crystalline symmetry, so we choose circular geometry for calculational convenience.

D_4-symmetric class-D HOTSC. For 2D D_4-symmetric systems with spinless fermions, there is an intriguing interacting 2D HOTSC with protected Majorana corner modes ξ_k and ξ_k' ($k = 1, 2, 3, 4$) that can be reformulated to complex fermions $c_k^\dagger = (\xi_k + i\xi_k')/\sqrt{2}$ (see Fig. 1). In this section we construct this phase by "almost free" coupled wires, with a necessary interaction only defined near the D_4 center. These Majorana

*jianhaozhang11@psu.edu

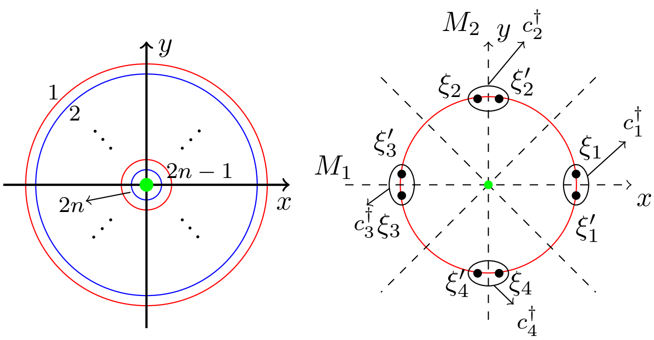

FIG. 1. Coupled-wire construction of 2D fermionic crystalline higher-order topological phases. Right panel: Dangling gapless modes of D_4-symmetric class-D or C_4-symmetric class-BDI HOTSCs. Dashed lines are reflection axes.

corner modes are also reformulated in terms of domain walls of 1D nonchiral Luttinger liquids [89]. Consider $2n$ decoupled 1D quantum wires with circular geometry (see Fig. 1), then the Lagrangian of the jth quantum wire is

$$\mathcal{L}_0^j = \frac{K_{IJ}^j}{4\pi}\left(\partial_\theta\phi_I^j\right)\left(\partial_t\phi_J^j\right) + \frac{V_{IJ}^j}{8\pi}\left(\partial_\theta\phi_I^j\right)\left(\partial_\theta\phi_J^j\right), \tag{1}$$

where $\phi^j = (\phi_1^j, \phi_2^j)^T$ is the two-component bosonic field of the jth quantum wire and $K^j = \sigma^z$ is the K matrix of the topological term [90]. The total Lagrangian of decoupled wires is $\mathcal{L}_0 = \sum_{j=1}^{2n} \mathcal{L}_0^j$. The D_4 symmetry properties of these bosonic fields are ($\boldsymbol{R} \in C_4/\boldsymbol{M}_1 \in \mathbb{Z}_2^M$ is the rotation/reflection generator of $D_4 = C_4 \rtimes \mathbb{Z}_2^M$ symmetry)

$$\begin{aligned}
\boldsymbol{R}: &\begin{cases} \phi_1^j(\theta) \mapsto -\phi_1^j(\theta + \pi/2), \\ \phi_2^j(\theta) \mapsto -\phi_2^j(\theta + \pi/2) + \pi, \end{cases} \\
\boldsymbol{M}_1: &\begin{cases} \phi_1^j(\theta) \mapsto -\phi_2^j(2\pi - \theta) + \pi/2, \\ \phi_2^j(\theta) \mapsto -\phi_1^j(2\pi - \theta) + \pi/2. \end{cases}
\end{aligned} \tag{2}$$

To figure out the Majorana corner modes of a D_4-symmetric HOTSC, we should further introduce the mass term with a domain-wall structure of each quantum wire,

$$\mathcal{L}_{\text{wall}}^j = m \sin(2\theta) \cos\left[\phi_1^j(\theta) + \phi_2^j(\theta)\right], \tag{3}$$

where $\mathcal{L}_{\text{wall}}^j$ is symmetric under Eq. (2), and $\mathcal{L}_{\text{wall}} = \sum_{j=1}^{2n} \mathcal{L}_{\text{wall}}^j$. For each quantum wire with a domain-wall structured mass term, there are four complex fermion zero modes at the poles $c_{1,2,3,4}^\dagger$ of the circle, with $\theta = 0, \pi/2, \pi, 3\pi/2$ because of the vanishing mass term, which are equivalent to eight MZMs. These dangling 0D gapless modes cannot be gapped in a D_4-symmetric way.

Subsequently we define two types of D_4-symmetric Eq. (2) interwire tunnelings that couple the $(2j-2+k)$th and $(2j-1+k)$th quantum wires ($m_1, m_2 < m$, $k = 1, 2$),

$$\mathcal{L}_{ck}^j = m_k \sum_{\alpha=1}^{2} \cos\left[\phi_\alpha^{2j-2+k}(\theta) - \phi_\alpha^{2j-1+k}(\theta)\right], \tag{4}$$

and $\mathcal{L}_{ck} = \sum_{j=1}^{n} \mathcal{L}_{ck}^j$. There are two extreme cases: $m_1 \neq 0$, $m_2 = 0/m_1 = 0$, $m_2 \neq 0$ correspond to the phase where $\mathcal{L}_{c1}/\mathcal{L}_{c2}$ dominates the interwire physics. For the $\mathcal{L}_{c1}$-dominant phase, the $(2j-1)$th and $2j$th wires are paired up and gapped, hence the corresponding system is fully gapped on a open circle and is topologically trivial.

For the $\mathcal{L}_{c2}$-dominant phase, the $2j$th and $(2j+1)$th wires are paired up and gapped, hence all 1D wires except the first and $2n$th are gapped. The first wire on the edge of the system presents four complex fermions/eight MZMs at the poles of the circle, which are exactly the second-order topological surface modes of a 2D D_4-symmetric class-D HOTSC. Near the D_4 center, there are also gapless modes on the $2n$th quantum wire. Distinct from quantum wires away from the D_4 center, the bosonic field ϕ^{2n} of the $2n$th quantum wires with different polar angles can tunnel to/interact with the field at other places. Consider two interacting terms of the $2n$th quantum wire near the D_4 center,

$$\mathcal{L}_{\text{int}} = m' \sum_{\beta=1}^{2} \cos\left(\sum_{\alpha=1}^{2}\left[\phi_\alpha^{2n}(\theta) - \phi_\alpha^{2n}(\beta\pi - \theta)\right]\right), \tag{5}$$

i.e., the intrawire couplings of the $2n$th wire lead to fully gapped bulks. Equivalently, a nontrivial 2D class-D D_4-symmetric HOTSC is described by 1D coupled wires with Lagrangian $\mathcal{L}_{D_4}^D = \mathcal{L}_0 + \mathcal{L}_{\text{wall}} + \mathcal{L}_{c2} + \mathcal{L}_{\text{int}}$. The intriguing interacting nature of this HOTSC is reflected by $\mathcal{L}_{\text{int}}$ near the D_4 center. On the other hand, the physics away from the D_4 center is well understood on a noninteracting level. The classification of a 2D class-D HOTSC is $\mathbb{Z}_2$, composed by phases dominated by interwire coupling $\mathcal{L}_{c1}$ and $\mathcal{L}_{c2}$ (see Fig. 5).

C_4-symmetric class-BDI HOTSC. For 2D BDI-class systems with C_4 symmetry, there is another type of intriguing interacting 2D HOTSC [45]. We construct these phases by "interacting" coupled wires in this section. Consider $4n$ 1D circular quantum wires, where each wire is described by Lagrangian Eq. (1) with $\phi^j = (\phi_1^j, \phi_2^j, \phi_3^j, \phi_4^j)^T$ as the four-component bosonic field of the jth quantum wire, $K^j = \sigma^z \oplus \sigma^z$ as the topological K matrix, and the total Lagrangian of all $4n$ 1D quantum wires is $\mathcal{L}_0 = \sum_{j=1}^{4n} \mathcal{L}_0^j$. The $(C_4 \times \mathbb{Z}_2^T)$-symmetry properties are defined as [90]

$$\boldsymbol{R}: \begin{cases} \phi_1^j \mapsto \phi_1^j + \phi_3^j - \phi_4^j - \pi/2, \\ \phi_2^j \mapsto \phi_2^j - \phi_3^j + \phi_4^j + \pi/2, \\ \phi_3^j \mapsto \phi_1^j + \phi_2^j - \phi_3^j + \pi/2, \\ \phi_4^j \mapsto \phi_1^j + \phi_2^j - \phi_4^j + \pi/2, \end{cases} \quad \theta \mapsto \theta + \pi/2, \tag{6}$$

$$\boldsymbol{T}: \begin{cases} \phi_1^j(\theta) \mapsto \phi_2^j(\theta) - \phi_3^j(\theta) + \phi_4^j(\theta), \\ \phi_2^j(\theta) \mapsto \phi_1^j(\theta) + \phi_3^j(\theta) - \phi_4^j(\theta) + \pi, \\ \phi_3^j(\theta) \mapsto \phi_1^j(\theta) + \phi_2^j(\theta) - \phi_4^j(\theta) + \pi, \\ \phi_4^j(\theta) \mapsto \phi_1^j(\theta) + \phi_2^j(\theta) - \phi_3^j(\theta). \end{cases} \tag{7}$$

Then we repeatedly figure out the Majorana corner modes by backscattering terms with a domain-wall structure: For each quantum wire, we introduce a symmetric [cf. Eqs. (6) and (7)] mass term

$$\mathcal{L}_{\text{wall}}^j = m \sum_{\alpha=1}^{2} \cos\left(\theta - \frac{\alpha\pi}{2}\right) \cos\left[\phi_\alpha^j(\theta) - \phi_{5-\alpha}^j(\theta)\right], \tag{8}$$

and $\mathcal{L}_{\text{wall}} = \sum_{j=1}^{4n} \mathcal{L}_{\text{wall}}^j$. For each quantum wire, there are four gapless complex fermions $c_k^\dagger$ (eight MZMs ξ_k and ξ_k') at the poles of the circle, where two of them at the north and south poles are from the first term of Eq. (8) and other two at the east and west poles are from the second term of Eq. (8). These dangling gapless modes cannot be gapped in a $(C_4 \times \mathbb{Z}_2^T)$-symmetric way.

Subsequently we consider $(C_4 \times \mathbb{Z}_2^T)$-symmetric [cf. Eqs. (6) and (7)] interwire interactions including four 1D quantum wires ($k = 1, 2, 3, 4$) [90],

$$\begin{aligned}\mathcal{L}_{ck}^j = m_k \sum_{\alpha=1}^{2} & \cos\left[\phi_\alpha^{4j-4+k} - \phi_{5-\alpha}^{4j-4+k} + \phi_\alpha^{4j-3+k} - \phi_{5-\alpha}^{4j-3+k}\right] \\ & + \cos\left[\phi_\alpha^{4j-4+k} - \phi_{5-\alpha}^{4j-4+k} + \phi_\alpha^{4j-2+k} - \phi_{5-\alpha}^{4j-2+k}\right] \\ & + \cos\left[\phi_\alpha^{4j-2+k} - \phi_{5-\alpha}^{4j-2+k} + \phi_\alpha^{4j-1+k} - \phi_{5-\alpha}^{4j-1+k}\right] \\ & + \cos\left[\phi_\alpha^{4j-3+k} - \phi_{5-\alpha}^{4j-3+k} + \phi_\alpha^{4j-1+k} - \phi_{5-\alpha}^{4j-1+k}\right],\end{aligned} \tag{9}$$

and the total Lagrangian of the interwire couplings is $\mathcal{L}_{ck} = \sum_{j=1}^{n-1} \mathcal{L}_{ck}^j$. There are four extreme cases: $m_k \neq 0$ ($k = 1, 2, 3, 4$) as the only nonzero index in $m_{1,2,3,4}$, which corresponds to the phase that $\mathcal{L}_{ck}$ that dominates the interwire physics. For the $\mathcal{L}_{c1}$-dominant phase, the $(4j - k)$th ($k = 0, 1, 2, 3$) quantum wires are assembled and gapped, hence the spectrum is fully gapped on a 2D open circle, and the corresponding phase is topologically trivial.

For the $\mathcal{L}_{c4}$-dominant phase with $m_4 \neq 0$ and $m_{1,2,3} = 0$, by applying $\mathcal{L}_{\text{wall}}$ and $\mathcal{L}_{c4}$, the $(4j + 3 - k)$th quantum wires are assembled and gapped, and there are only four quantum wires remaining gapless: the first, second, third on the edge, and $4n$th near the C_4 center. On the edge, the first, second, and third quantum wires with dangling gapless modes are treated as the higher-order edge state of the 2D C_4-symmetric class-BDI HOTSC; near the C_4 center, in order to obtain a HOTSC, we should further add some intrawire interactions to fully gap the $4n$th quantum wire in order to get a fully gapped bulk state. Consider the four-body interacting terms of a $4n$th quantum wire, composed of the backscatterings of bosonic fields $\phi_{1,2,3,4}^{4n}$ with different polar angles [90],

$$\begin{aligned}\mathcal{L}_{\text{int}} = m' \sum_{\alpha,\beta=1}^{2} & \cos\left[\phi_\alpha^{4n}(\theta) - \phi_{5-\alpha}^{4n}(\theta) + \phi_\alpha^{4n}(\theta + \beta\pi/2)\right. \\ & \left. - \phi_{5-\alpha}^{4n}(\theta + \beta\pi/2)\right],\end{aligned} \tag{10}$$

i.e., the intrawire interactions of the $4n$th quantum wire lead to a fully gapped bulk, and a nontrivial 2D $(C_4 \times \mathbb{Z}_2^T)$-symmetric HOTSC with spinless fermions is described by 1D coupled quantum wires with Lagrangian $\mathcal{L}_{C_4}^{\text{BDI}} = \mathcal{L}_0 + \mathcal{L}_{\text{wall}} + \mathcal{L}_{c4} + \mathcal{L}_{\text{int}}$. Similar for the $\mathcal{L}_{c2}$- and $\mathcal{L}_{c3}$-dominant phases, there are four topologically distinct phases for a 2D BDI-class $(C_4 \times \mathbb{Z}_2^T)$-symmetric system (see Fig. 2). The interacting nature of these topological phases is reflected by interwire interactions $\mathcal{L}_{ck}$ and intrawire interactions near the C_4 center, $\mathcal{L}_{\text{int}}$. The classification of a 2D class-BDI HOTSC is $\mathbb{Z}_4$, composed of phases dominated by interwire couplings $\mathcal{L}_{ck}$ ($k = 1, 2, 3, 4$).

The coupled-wire construction is not limited to superconductors, but it is also applicable to topological insulators: the only difference is that the Luttinger liquid Eq. (1) should respect the $U(1)$ charge conservation.

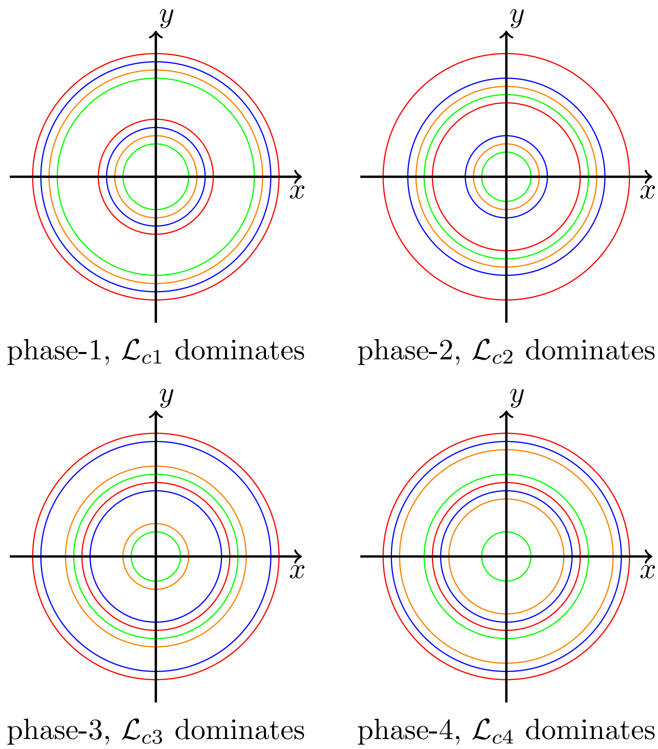

FIG. 2. Four distinct phases of a 2D BDI-class $(C_4 \times \mathbb{Z}_2^T)$-symmetric system. Each of the four 1D wires with narrower intervals can be gapped by interwire interactions $\mathcal{L}_{ck}$, and the 1D wire near the C_4 center can be gapped by intrawire interactions $\mathcal{L}_{\text{int}}$.

Imposition of lattice translation. With point group symmetric cases, using a D_4-symmetric class-D example, we demonstrate that the imposition of lattice translation symmetry is straightforward: We impose the lattice translation to D_4 leads to the $p4mm$ wallpaper group. We arrange eight quantum wires near each D_4 center (four vertical and four horizontal—see Fig. 3), where different topological phases are also controlled by patterns of interwire couplings: The topologically trivial phase is dominated by $\mathcal{L}_{c1}$ (black double arrows in Fig. 3), and the nontrivial phase is dominated by $\mathcal{L}_{c2}$ (red double arrows in Fig. 3) and $\mathcal{L}_{\text{int}}$ at each D_4 center in order to the fully gapped bulk.

Quantum phase transition of HOTSC. The coupled-wire picture serves as a unique platform for investigating the quantum phase transition (QPT) of 2D HOTSCs because of its clear formulations. In this section, we elucidate the QPT of a 2D intriguing interacting D_4-symmetric HOTSC as a representative example. Consider the D_4-symmetric Lagrangian $\mathcal{L}_0 + \mathcal{L}_{c1} + \mathcal{L}_{c2} + \mathcal{L}_{\text{int}}$, where above we have discussed two extreme cases with $m_1 = 0/m_2 = 0$, derived two distinct phases characterized by the appearance of Majorana corner modes on the edge (first quantum wire). Now we suppose $m = 10m_1$ and set both m_1 and m_2 finite and study the possible QPT by tuning their ratio m_2/m_1. As summarized in Fig. 4, when we turn on m_2 in the $m_2 < m_1$ regime, the system remains fully gapped with a narrower gap; at $m_1 = m_2$, the gap

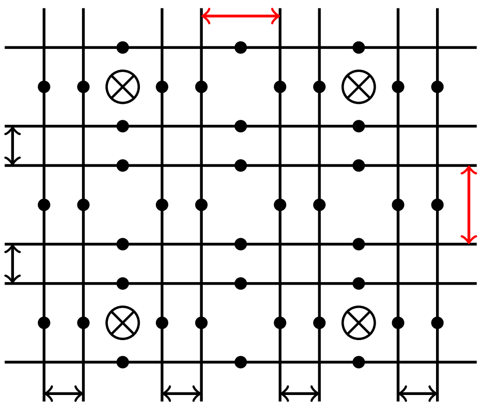

FIG. 3. Coupled wires of a 2D $p4mm$-symmetric class-D HOTSC. Each "$\otimes$" symbol depicts a center of D_4, each line (horizontal or vertical) depicts a quantum wire, and each dot depicts a domain wall described by $\mathcal{L}^j_{\text{wall}}$. Red and black double arrows depict different interwire couplings $\mathcal{L}_{c1}$ and $\mathcal{L}_{c2}$.

closes and the system becomes critical; as we keep increasing m_2 toward the $m_2 > m_1$ regime, the system reopens a *bulk* gap but leaves several gapless modes on the edge, which are exactly the Majorana domain walls of a 1D quantum wire on the edge. Therefore, we conclude that there is a clear quantum phase transition from a trivial state to a 2D D_4-symmetric HOTSC at the $m_1 = m_2$ point. Equivalently, this quantum phase transition is characterized by different interwire entanglement patterns of 1D quantum wires, as illustrated in Fig. 5.

For a 2D C_4-symmetric class-BDI system, the quantum phase transitions can be described in a similar way with little complications. For this case, there are four distinct phases controlled by four different parameters $m_{1,2,3,4}$ (see Fig. 2). As an example, for the quantum phase transition between phase 2 and phase 3, we set $m_1 = m_4 = 0$ and investigate the bulk gap by tuning the ratio m_2/m_3. Heuristically, we see that the system will be critical for $m_2 = m_3$, hence there will be a quantum phase transition at this point [90]. As a matter of fact, distinct phases of 2D HOTSC are controlled by different patterns of interwire entanglements, and their quantum phase transitions can be manipulated by tuning the intensities of different types of interwire couplings. In other words, a coupled-wire construction provides a straightforward way of comprehending the quantum phase transitions of 2D HOTSCs, by tuning the interwire couplings to control the

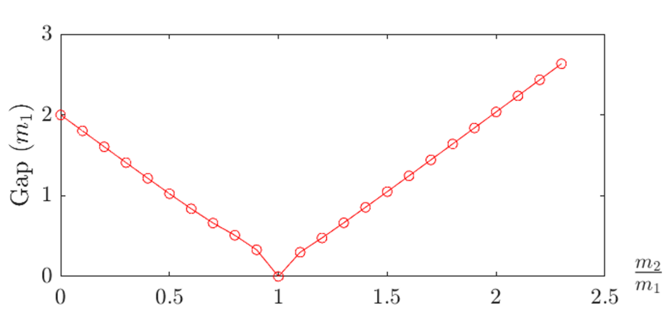

FIG. 4. Bulk gap of 2D D_4-symmetric Lagrangian $\mathcal{L}_0 + \mathcal{L}_{c1} + \mathcal{L}_{c2} + \mathcal{L}_{\text{int}}$, with respect to the ratio m_2/m_1.

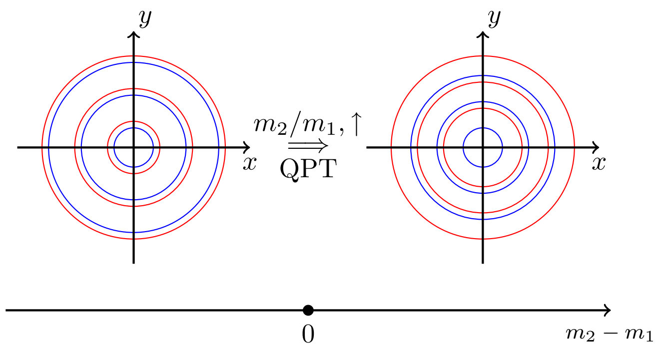

FIG. 5. Quantum phase transition of a 2D D_4-symmetric HOTSC, with respect to $m_2 - m_1$. Each pair of quantum wires with narrower intervals is coupled.

patterns of interwire entanglement. Different phases are manifested by different numbers of Majorana zero modes at each pole of the outermost quantum wire.

Experimental implications. In this Letter, the explicit manifestations of second-order modes on the edges of the systems by domain-wall structured quantum wires serve as a direct opportunity for observing the higher-order topological phases by tunneling spectroscopic measurements. Recently, the coupled-wire picture was straightforwardly manifested in two-dimensional moiré superlattices [91,92]. In particular, in Ref. [92], one-dimensional Luttinger liquid behavior has been explicitly observed in a 2D bilayer WTe_2 moiré superlattice by direct transport measurements. Hence our approach can be applied directly to moiré superlattices.

Conclusion and discussion. The coupled-wire construction is a celebrated aspect in topological phases of quantum matter, for both long-range and short-range entangled systems. In this Letter, we establish the coupled-wire construction of a 2D intriguing interacting fermionic crystalline HOTSC, with two representative examples: 2D D_4-symmetric class-D and C_4-symmetric class-BDI HOTSC phases. An indispensable advantage of the coupled-wire construction is that the powerful bosonization technique can be utilized, and the interwire couplings can be straightforwardly involved by many-body backscattering terms in the Lagrangian. With this advantage, we use a 1D nonchiral Luttinger liquid with a domain-wall structured mass term as an "almost gapped" 1D quantum wire. Based on these quantum wires, we introduce some suitable interwire couplings in order to gap out the bulk by assemblies of quantum wires. The remaining ungapped quantum wires on the edge are treated as the edge theory of 2D HOTSCs. Near the center of the point group, the ungapped quantum wires are gapped by interactions of bosonic fields at different places. The lattice translation symmetry can be straightforwardly imposed. Distinct HOTSCs are manifested by different patterns of interwire entanglement. Furthermore, the concrete coupled-wire constructions serve as a straightforward way to comprehend the quantum phase transitions of 2D HOTSCs, by directly tuning the interwire couplings to control the interwire entanglement patterns. The coupled-wire construction can also be generalized to the systems with arbitrary crystalline symmetry SG and internal symmetry G_0 in arbitrary dimensions, and especially in 2D moiré superlattices, with more complicated interwire entanglement patterns, and their quantum phase transitions should also be controlled by the interwire entanglement patterns of the quantum wires. Furthermore, with explicit corner modes, the 2D HOTSC may be directly justified by tunneling spectroscopic measurements on the edge.

Acknowledgments. The author thanks Meng Cheng, Shang-Qiang Ning, Liujun Zou, and Rui-Xing Zhang for stimulating discussions. This work is supported by Direct Grant No. 4053462 from The Chinese University of Hong Kong and funding from Hong Kong's Research Grants Council (GRF No. 14306420, ANR/RGC Joint Research Scheme No. A-CUHK402/18).

[1] D. C. Tsui, H. L. Stormer, and A. C. Gossard, Two-Dimensional Magnetotransport in the Extreme Quantum Limit, Phys. Rev. Lett. **48**, 1559 (1982).
[2] R. B. Laughlin, Anomalous Quantum Hall Effect: An Incompressible Quantum Fluid with Fractionally Charged Excitations, Phys. Rev. Lett. **50**, 1395 (1983).
[3] X. Chen, Z.-C. Gu, and X.-G. Wen, Local unitary transformation, long-range quantum entanglement, wave function renormalization, and topological order, Phys. Rev. B **82**, 155138 (2010).
[4] Z.-C. Gu and X.-G. Wen, Tensor-entanglement-filtering renormalization approach and symmetry-protected topological order, Phys. Rev. B **80**, 155131 (2009).
[5] X. Chen, Z.-C. Gu, and X.-G. Wen, Classification of gapped symmetric phases in one-dimensional spin systems, Phys. Rev. B **83**, 035107 (2011).
[6] X. Chen, Z.-C. Gu, Z.-X. Liu, and X.-G. Wen, Symmetry-protected topological orders in interacting bosonic systems, Science **338**, 1604 (2012).
[7] X. Chen, Z.-C. Gu, Z.-X. Liu, and X.-G. Wen, Symmetry protected topological orders and the group cohomology of their symmetry group, Phys. Rev. B **87**, 155114 (2013).
[8] T. Senthil, Symmetry-protected topological phases of quantum matter, Annu. Rev. Condens. Matter Phys. **6**, 299 (2015).
[9] E. Plamadeala, M. Mulligan, and C. Nayak, Short-range entangled bosonic states with chiral edge modes and T duality of heterotic strings, Phys. Rev. B **88**, 045131 (2013).
[10] Y.-M. Lu and A. Vishwanath, Theory and classification of interacting integer topological phases in two dimensions: A Chern-Simons approach, Phys. Rev. B **86**, 125119 (2012).
[11] D. S. Freed, Short-range entanglement and invertible field theories, arXiv:1406.7278.
[12] D. S. Freed and M. J. Hopkins, Reflection positivity and invertible topological phases, Geom. Topol. **25**, 1165 (2021).
[13] Z.-C. Gu and X.-G. Wen, Symmetry-protected topological orders for interacting fermions: Fermionic topological nonlinear σ models and a special group supercohomology theory, Phys. Rev. B **90**, 115141 (2014).
[14] Q.-R. Wang and Z.-C. Gu, Towards a Complete Classification of Symmetry-Protected Topological Phases for Interacting Fermions in Three Dimensions and a General Group Supercohomology Theory, Phys. Rev. X **8**, 011055 (2018).
[15] Q.-R. Wang and Z.-C. Gu, Construction and Classification of Symmetry-Protected Topological Phases in Interacting Fermion Systems, Phys. Rev. X **10**, 031055 (2020).
[16] A. Kapustin, Symmetry protected topological phases, anomalies, and cobordisms: Beyond group cohomology, arXiv:1403.1467.
[17] A. Kapustin, R. Thorngren, A. Turzillo, and Z. Wang, Fermionic symmetry protected topological phases and cobordisms, J. High Energy Phys. 12 (2015) 052.
[18] A. Kapustin and R. Thorngren, Fermionic SPT phases in higher dimensions and bosonization, J. High Energy Phys. 10 (2017) 080.
[19] Z.-C. Gu and M. Levin, Effect of interactions on two-dimensional fermionic symmetry-protected topological phases with Z_2 symmetry, Phys. Rev. B **89**, 201113(R) (2014).
[20] M. Cheng and Z.-C. Gu, Topological Response Theory of Abelian Symmetry-Protected Topological Phases in Two Dimensions, Phys. Rev. Lett. **112**, 141602 (2014).
[21] M. Barkeshli, P. Bonderson, M. Cheng, and Z. Wang, Symmetry fractionalization, defects, and gauging of topological phases, Phys. Rev. B **100**, 115147 (2019).
[22] N. Tantivasadakarn, Dimensional reduction and topological invariants of symmetry-protected topological phases, Phys. Rev. B **96**, 195101 (2017).
[23] C. Wang, C.-H. Lin, and Z.-C. Gu, Interacting fermionic symmetry-protected topological phases in two dimensions, Phys. Rev. B **95**, 195147 (2017).
[24] M. Cheng, Z. Bi, Y.-Z. You, and Z.-C. Gu, Classification of symmetry-protected phases for interacting fermions in two dimensions, Phys. Rev. B **97**, 205109 (2018).
[25] M. Cheng, N. Tantivasadakarn, and C. Wang, Loop Braiding Statistics and Interacting Fermionic Symmetry-Protected Topological Phases in Three Dimensions, Phys. Rev. X **8**, 011054 (2018).
[26] S.-Q. Ning, C. Wang, Q.-R. Wang, and Z.-C. Gu, Edge theories of two-dimensional fermionic symmetry protected topological phases protected by unitary Abelian symmetries, Phys. Rev. B **104**, 075151 (2021).
[27] M. Z. Hasan and C. L. Kane, Colloquium: Topological insulators, Rev. Mod. Phys. **82**, 3045 (2010).
[28] X.-L. Qi and S.-C. Zhang, Topological insulators and superconductors, Rev. Mod. Phys. **83**, 1057 (2011).
[29] L. Fu, Topological Crystalline Insulators, Phys. Rev. Lett. **106**, 106802 (2011).
[30] T. H. Hsieh, H. Lin, J. Liu, W. Duan, A. Bansil, and L. Fu, Topological crystalline insulators in the SnTe material class, Nat. Commun. **3**, 982 (2012).
[31] H. Isobe and L. Fu, Theory of interacting topological crystalline insulators, Phys. Rev. B **92**, 081304(R) (2015).
[32] H. Song, S.-J. Huang, L. Fu, and M. Hermele, Topological Phases Protected by Point Group Symmetry, Phys. Rev. X **7**, 011020 (2017).
[33] S.-J. Huang, H. Song, Y.-P. Huang, and M. Hermele, Building crystalline topological phases from lower-dimensional states, Phys. Rev. B **96**, 205106 (2017).

[34] R. Thorngren and D. V. Else, Gauging Spatial Symmetries and the Classification of Topological Crystalline Phases, Phys. Rev. X **8**, 011040 (2018).
[35] L. Zou, Bulk characterization of topological crystalline insulators: Stability under interactions and relations to symmetry enriched $U(1)$ quantum spin liquids, Phys. Rev. B **97**, 045130 (2018).
[36] H. C. Po, A. Vishwanath, and H. Watanabe, Symmetry-based indicators of band topology in the 230 space groups, Nat. Commun. **8**, 50 (2017).
[37] H. Song, C. Z. Xiong, and S.-J. Huang, Bosonic crystalline symmetry protected topological phases beyond the group cohomology proposal, Phys. Rev. B **101**, 165129 (2020).
[38] S. Jiang and Y. Ran, Anyon condensation and a generic tensor-network construction for symmetry-protected topological phases, Phys. Rev. B **95**, 125107 (2017).
[39] J. Kruthoff, J. de Boer, J. van Wezel, C. L. Kane, and R.-J. Slager, Topological Classification of Crystalline Insulators through Band Structure Combinatorics, Phys. Rev. X **7**, 041069 (2017).
[40] K. Shiozaki, M. Sato, and K. Gomi, Atiyah-Hirzebruch spectral sequence in band topology: General formalism and topological invariants for 230 space groups, arXiv:1802.06694.
[41] Z. Song, S.-J. Huang, Y. Qi, C. Fang, and M. Hermele, Topological states from topological crystals, Sci. Adv. **5**, eaax2007 (2019).
[42] D. V. Else and R. Thorngren, Crystalline topological phases as defect networks, Phys. Rev. B **99**, 115116 (2019).
[43] Z. Song, C. Fang, and Y. Qi, Real-space recipes for general topological crystalline states, Nat. Commun. **11**, 4197 (2020).
[44] K. Shiozaki, C. Z. Xiong, and K. Gomi, Generalized homology and Atiyah-Hirzebruch spectral sequence in crystalline symmetry protected topological phenomena, arXiv:1810.00801.
[45] M. Cheng and C. Wang, Rotation symmetry-protected topological phases of fermions, Phys. Rev. B **105**, 195154 (2022).
[46] J.-H. Zhang, Q.-R. Wang, S. Yang, Y. Qi, and Z.-C. Gu, Construction and classification of point-group symmetry-protected topological phases in two-dimensional interacting fermionic systems, Phys. Rev. B **101**, 100501(R) (2020).
[47] A. Rasmussen and Y.-M. Lu, Classification and construction of higher-order symmetry protected topological phases of interacting bosons, Phys. Rev. B **101**, 085137 (2020).
[48] A. Rasmussen and Y.-M. Lu, Intrinsically interacting topological crystalline insulators and superconductors, arXiv:1810.12317.
[49] M. Cheng, Fermionic Lieb-Schultz-Mattis theorems and weak symmetry-protected phases, Phys. Rev. B **99**, 075143 (2019).
[50] S.-J. Huang and M. Hermele, Surface field theories of point group symmetry protected topological phases, Phys. Rev. B **97**, 075145 (2018).
[51] S. Ono, H. C. Po, and K. Shiozaki, $\mathbb{Z}_2$-enriched symmetry indicators for topological superconductors in the 1651 magnetic space groups, Phys. Rev. Research **3**, 023086 (2021).
[52] S.-J. Huang, 4D beyond-cohomology topological phase protected by C_2 symmetry and its boundary theories, Phys. Rev. Research **2**, 033236 (2020).
[53] S.-J. Huang and Y.-T. Hsu, Faithful derivation of symmetry indicators: A case study for topological superconductors with time-reversal and inversion symmetries, Phys. Rev. Research **3**, 013243 (2021).
[54] J.-H. Zhang, S. Yang, Y. Qi, and Z.-C. Gu, Real-space construction of crystalline topological superconductors and insulators in 2D interacting fermionic systems, arXiv:2012.15657.
[55] J.-H. Zhang and S. Yang, Tensor network representations of fermionic crystalline topological phases on two-dimensional lattices, arXiv:2109.06118.
[56] N. Manjunath and M. Barkeshli, Crystalline gauge fields and quantized discrete geometric response for Abelian topological phases with lattice symmetry, Phys. Rev. Research **3**, 013040 (2021).
[57] M. Barkeshli, Y.-A. Chen, P.-S. Hsin, and N. Manjunath, Classification of (2+1)D invertible fermionic topological phases with symmetry, Phys. Rev. B **105**, 235143 (2022).
[58] L. Fidkowski, A. Vishwanath, and M. A. Metlitski, Surface topological order and a new 't Hooft anomaly of interaction enabled 3+1D fermion SPTs, arXiv:1804.08628.
[59] J. Sullivan and M. Cheng, Interacting edge states of fermionic symmetry-protected topological phases in two dimensions, SciPost Phys. **9**, 016 (2020).
[60] J.-H. Zhang, Y. Qi, and Z.-C. Gu, Construction and classification of crystalline topological superconductor and insulators in three-dimensional interacting fermion systems, arXiv:2204.13558.
[61] Y. Tanaka, Z. Ren, T. Sato, K. Nakayama, S. Souma, T. Takahashi, K. Segawa, and Y. Ando, Experimental realization of a topological crystalline insulator in SnTe, Nat. Phys. **8**, 800 (2012).
[62] P. Dziawa, B. J. Kowalski, K. Dybko, R. Buczko, A. Szczerbakow, M. Szot, E. Łusakowska, T. Balasubramanian, B. M. Wojek, M. H. Berntsen, O. Tjernberg, and T. Story, Topological crystalline insulator states in $Pb_{1-x}Sn_xSe$, Nat. Mater. **11**, 1023 (2012).
[63] Y. Okada, M. Serbyn, H. Lin, D. Walkup, W. Zhou, C. Dhital, M. Neupane, S. Xu, Y. J. Wang, R. Sankar, F. Chou, A. Bansil, M. Z. Hasan, S. D. Wilson, L. Fu, and V. Madhavan, Observation of Dirac node formation and mass acquisition in a topological crystalline insulator, Science **341**, 1496 (2013).
[64] J. Ma, C. Yi, B. Lv, Z. Wang, S. Nie, L. Wang, L. Kong, Y. Huang, P. Richard, P. Zhang, K. Yaji, K. Kurado, S. Shin, H. Weng, B. A. Bernevig, Y. Shi, T. Qian, and H. Ding, Experimental evidence of hourglass fermion in the candidate nonsymmorphic topological insulator khgsb, Sci. Adv. **3**, e1602415 (2017).
[65] Q. Wang, C.-C. Liu, Y.-M. Lu, and F. Zhang, High-Temperature Majorana Corner States, Phys. Rev. Lett. **121**, 186801 (2018).
[66] Z. Yan, F. Song, and Z. Wang, Majorana Corner Modes in a High-Temperature Platform, Phys. Rev. Lett. **121**, 096803 (2018).
[67] T. Liu, J. J. He, and F. Nori, Majorana corner states in a two-dimensional magnetic topological insulator on a high-temperature superconductor, Phys. Rev. B **98**, 245413 (2018).
[68] Y. Wang, M. Lin, and T. L. Hughes, Weak-pairing higher order topological superconductors, Phys. Rev. B **98**, 165144 (2018).
[69] H. Shapourian, Y. Wang, and S. Ryu, Topological crystalline superconductivity and second-order topological superconductivity in nodal-loop materials, Phys. Rev. B **97**, 094508 (2018).
[70] R.-X. Zhang, W. S. Cole, and S. D. Sarma, Helical Hinge Majorana Modes in Iron-Based Superconductors, Phys. Rev. Lett. **122**, 187001 (2019).

[71] C.-H. Hsu, P. Stano, J. Klinovaja, and D. Loss, Majorana Kramers Pairs in Higher-Order Topological Insulators, Phys. Rev. Lett. **121**, 196801 (2018).

[72] N. Bultinck, B. A. Bernevig, and M. P. Zaletel, Three-dimensional superconductors with hybrid higher-order topology, Phys. Rev. B **99**, 125149 (2019).

[73] B. Roy, Higher-order topological superconductors in $\mathcal{P}$-, $\mathcal{T}$-odd quadrupolar Dirac materials, Phys. Rev. B **101**, 220506(R) (2020).

[74] B. Roy and V. Juričić, Mixed-parity octupolar pairing and corner Majorana modes in three dimensions, Phys. Rev. B **104**, L180503 (2021).

[75] K. Laubscher, D. Loss, and J. Klinovaja, Fractional topological superconductivity and parafermion corner states, Phys. Rev. Research **1**, 032017(R) (2019).

[76] K. Laubscher, D. Loss, and J. Klinovaja, Majorana and parafermion corner states from two coupled sheets of bilayer graphene, Phys. Rev. Research **2**, 013330 (2020).

[77] E. J. Bergholtz and A. Karlhede, Quantum Hall system in Tao-Thouless limit, Phys. Rev. B **77**, 155308 (2008).

[78] C. L. Kane, R. Mukhopadhyay, and T. C. Lubensky, Fractional Quantum Hall Effect in an Array of Quantum Wires, Phys. Rev. Lett. **88**, 036401 (2002).

[79] J. C. Y. Teo and C. L. Kane, From Luttinger liquid to non-Abelian quantum hall states, Phys. Rev. B **89**, 085101 (2014).

[80] Y. Fuji and P. Lecheminant, Non-Abelian $SU(N-1)$-singlet fractional quantum Hall states from coupled wires, Phys. Rev. B **95**, 125130 (2017).

[81] T. Meng, T. Neupert, M. Greiter, and R. Thomale, Coupled-wire construction of chiral spin liquids, Phys. Rev. B **91**, 241106(R) (2015).

[82] E. Sagi and Y. Oreg, From an array of quantum wires to three-dimensional fractional topological insulators, Phys. Rev. B **92**, 195137 (2015).

[83] I. Seroussi, E. Berg, and Y. Oreg, Topological superconducting phases of weakly coupled quantum wires, Phys. Rev. B **89**, 104523 (2014).

[84] T. Iadecola, T. Neupert, C. Chamon, and C. Mudry, Wire constructions of Abelian topological phases in three or more dimensions, Phys. Rev. B **93**, 195136 (2016).

[85] T. Neupert, C. Chamon, C. Mudry, and R. Thomale, Wire deconstructionism of two-dimensional topological phases, Phys. Rev. B **90**, 205101 (2014).

[86] J. Klinovaja and Y. Tserkovnyak, Quantum spin Hall effect in strip of stripes model, Phys. Rev. B **90**, 115426 (2014).

[87] J. Klinovaja, Y. Tserkovnyak, and D. Loss, Integer and fractional quantum anomalous Hall effect in a strip of stripes model, Phys. Rev. B **91**, 085426 (2015).

[88] J. Klinovaja and D. Loss, Integer and fractional quantum Hall effect in a strip of stripes, Eur. Phys. J. B **87**, 171 (2014).

[89] J.-H. Zhang and S.-Q. Ning, Crystalline equivalent boundary-bulk correspondence of two-dimensional topological phases, arXiv:2112.14567.

[90] See Supplemental Materials at http://link.aps.org/supplemental/10.1103/PhysRevB.106.L020503 for more details, which includes a reference to F. D. M. Haldane, Stability of Chiral Luttinger Liquids and Abelian Quantum Hall States, Phys. Rev. Lett. **74**, 2090(1995).

[91] X.-C. Wu, C.-M. Jian, and C. Xu, Coupled-wire description of the correlated physics in twisted bilayer graphene, Phys. Rev. B **99**, 161405(R) (2019).

[92] P. Wang, G. Yu, Y. H. Kwan, Y. Jia, S. Lei, S. Klemenz, F. A. Cevallos, R. Singha, T. Devakul, K. Watanabe, T. Taniguchi, S. L. Sondhi, R. J. Cava, L. M. Schoop, S. A. Parameswaran, and S. Wu, One-dimensional Luttinger liquids in a two-dimensional moiré lattice, Nature (London) **605**, 57 (2022).